

****TITLE****
*ASP Conference Series, Vol. **VOLUME***, ***YEAR OF PUBLICATION***
****NAMES OF EDITORS****

SAURON Observations of Disks in Spheroids

M. Bureau

*Columbia Astrophysics Laboratory, 550 W. 120th St., 1027 Pupin Hall,
Mail Code 5247, New York NY 10027, USA*

R. Bacon, E. Emsellem

CRAL, 9 Avenue Charles-André, 69230 Saint-Genis-Laval, France

M. Cappellari, E.K. Verolme, P.T. de Zeeuw

Sterrewacht Leiden, Niels Bohrweg 2, 2333 CA Leiden, Netherlands

Y. Copin

*Institut de Physique Nucleaire de Lyon, 4 rue Enrico Fermi, 69622
Villeurbanne cedex, France*

R.L. Davies, R. McDermid

*Physics Department, University of Durham, South Road, Durham
DH1 3LE, UK*

H. Kuntschner

ESO, Karl-Schwarzschild-Str. 2, 85748 Garching, Germany

B.W. Miller

Gemini Observatory, Casilla 603, La Serena, Chile

R.F. Peletier

*Department of Physics and Astronomy, University of Nottingham,
University Park, Nottingham NG7 2RD, UK*

Abstract. The panoramic integral-field spectrograph SAURON is currently being used to map the stellar kinematics, gaseous kinematics, and stellar populations of a large number of early-type galaxies and bulges. Here, we describe SAURON observations of cold stellar disks embedded in spheroids (NGC 3384, NGC 4459, NGC 4526), we illustrate the kinematics and ionization state of large-scale gaseous disks (NGC 4278, NGC 7742), and we show preliminary comparisons of SAURON data with barred galaxy N-body simulations (NGC 3623).

1. Introduction

The physical properties of early-type galaxies correlate with luminosity and environment, as exemplified by the morphology-density relation (Dressler 1980) and the dependence of color, metal content, isophotal shape, nuclear cusp slope, and dynamical support on luminosity (e.g. Bender & Nieto 1990; Faber et al. 1997). It is unclear to what extent these properties were acquired at the epoch of galaxy formation or result from subsequent dynamical evolution.

Progress toward answering these and related issues requires a systematic investigation of the kinematics and line-strengths of a representative sample of early-type galaxies. The intrinsic shape, internal orbital structure, and radial dependence of the mass-to-light ratio are constrained by the stellar and gas kinematics (e.g. van der Marel & Franx 1993; Cretton, Rix, & de Zeeuw 2000); the age and metallicity of the stellar populations are constrained by the absorption line-strengths (Gonzalez 1993; Davies, Sadler, & Peletier 1993). SAURON contributions to these two complementary approaches are discussed in turn by Bacon et al. (2002) and Emsellem et al. (2002) in these proceedings.

Here, we focus on the importance of disks in spheroids. In the current context of hierarchical (i.e. merger-driven) structure formation, the dichotomy in the properties of early-type galaxies (e.g. Faber et al. 1997) is often explained by the mass ratio of the progenitor galaxies (e.g. Barnes 1998; Naab, Burkert, & Hernquist 1999). However, as revealed by SAURON, the presence of cold disks in a large number of spheroids suggests a non-negligible role for dissipation, reminiscent of the old galaxy formation debate between merging (Searle & Zinn 1978) and dissipational collapse (Eggen, Lynden-Bell, & Sandage 1962).

After reviewing the core properties of the SAURON instrument and sample (§ 2), we present in § 3 SAURON observations of a few cold central stellar disks embedded spheroids. We also illustrate the emission line distributions and kinematics of large-scale gaseous disks in § 4, and compare generic N-body simulations of barred galaxies with SAURON data in § 5.

2. SAURON: Instrument and Survey

SAURON (Spectrographic Areal Unit for Research on Optical Nebulae) is a panoramic integral-field spectrograph optimized for studies of the large-scale kinematics and stellar populations of spheroids (Bacon et al. 2001, hereafter Paper I). In its low-resolution mode, it has a $41'' \times 33''$ field-of-view sampled with $0''.94 \times 0''.94$ lenslets, 100% coverage, and high throughput. The spectra cover 4810–5350 Å with simultaneous sky subtraction. Stellar kinematic information is derived from the *Mgb* triplet and the Fe lines. The [OIII], $H\beta$, and [NI] emission lines provide the morphology, kinematics, and limited information on the ionization state of the ionized gas. The *Mgb*, $H\beta$, and Fe5270 absorption lines constrain the age and metallicity of the stellar populations.

The SAURON survey targets a representative sample of 72 nearby ellipticals, lenticulars, and early-type bulges constructed to be as free of biases as possible while ensuring the existence of complementary data (preferably space-based; $M_B \leq -18$). The galaxies are further split into “cluster” and “field” objects and populate the six $\epsilon - M_B$ planes uniformly (de Zeeuw et al. 2002, hereafter Paper II). By construction, the sample covers the full range of environment, flattening, rotational support, nuclear cusp slope, isophotal shape, etc.

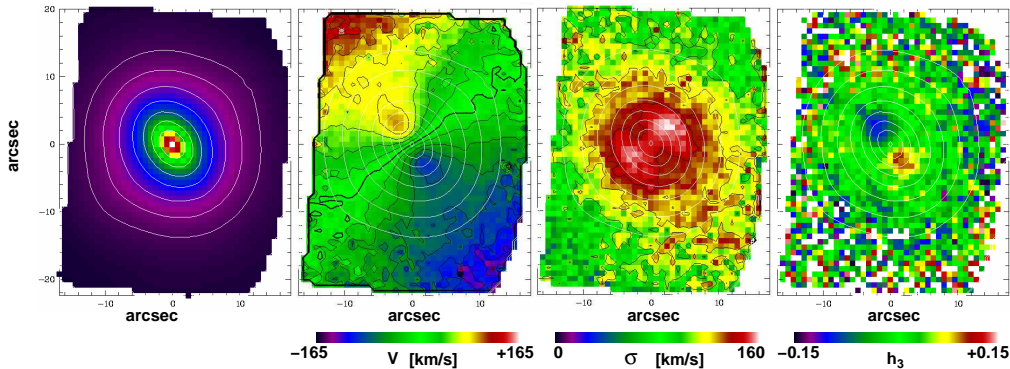


Figure 1. SAURON absorption-line measurements of the SB0 galaxy NGC 3384, based on a single pointing of 4×1800 s. The effective spatial sampling is $0''.8 \times 0''.8$ and the seeing was $\approx 2''.5$. a) Reconstructed total intensity I . b) Mean stellar velocity V . c) Stellar velocity dispersion σ . d) Gauss-Hermite moment h_3 . The Gauss-Hermite moment h_4 displays little variation and is not shown. Isophotes are overlaid for reference.

3. Stellar Disks Embedded in Spheroids

We discuss below the stellar kinematics of 3 galaxies showing the presence of a central stellar disk with varying strengths. The SAURON strategy is to map galaxies to one effective radius R_e , which for nearly half the sample requires only one pointing. For the largest galaxies, mosaics of two or three pointings reach $0.5 R_e$ only. The mean stellar velocity V , the velocity dispersion σ , and the Gauss-Hermite moments h_3 and h_4 (e.g. van der Marel & Franx 1993) are derived using the FCQ method (Bender 1990).

3.1. NGC 3384

NGC 3384 is a large SB0⁻(s) galaxy in the Leo I group ($M_B = -19.6$). It forms a triple on the sky with NGC 3379 and NGC 3389 but there is only marginal evidence for interactions. The light distribution in the central $\approx 20''$ is complex. The inner isophotes are elongated along the major axis, suggesting an embedded disk, but beyond $10''$ the elongation is along the minor-axis (e.g. Busarello et al. 1996). The isophotes are off-centered at much larger radii. NGC 3384 shows no emission lines, remains undetected in HI, CO, radio continuum, and X-ray, but has IRAS detections at 12 and $100 \mu\text{m}$ (e.g. Roberts et al. 1991).

Figure 1 displays the stellar kinematics of NGC 3384 and illustrates a key advantage of SAURON. Summing the flux in wavelength, the galaxy surface brightness distribution is recovered and there is no doubt about the relative location of the measurements. Figure 1 shows that the bulge of NGC 3384 rotates regularly. Mean velocities increase steeply along the major axis up to $r \approx 4''$, then decrease slightly, and rise again. No velocity gradient is observed along the minor axis. The velocity dispersion map shows a symmetric dumb-bell structure and the h_3 map is anti-correlated with V also within $r \approx 4''$ (see Fisher 1997). All these facts point to the presence of a cold, central stellar disk in NGC 3384.

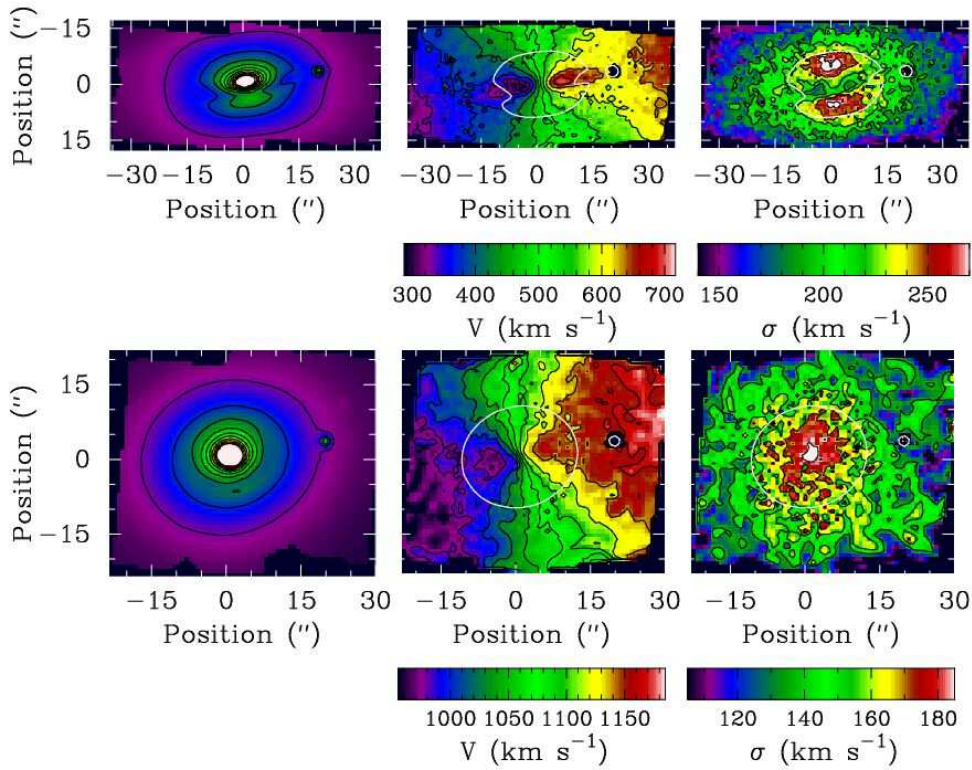


Figure 2. SAURON absorption-line measurements of the SB0 galaxies NGC 4526 and NGC 4459, both based on two overlapping pointings. Top row: Reconstructed total intensity, mean stellar velocity, and velocity dispersion fields of NGC 4526. Bottom row: Same for NGC 4459.

3.2. NGC 4526 and NGC 4459

Many other galaxies in our sample show evidence of a central stellar disk. NGC 3623 is discussed in Paper II. Figure 2 shows two cases where the disk appears to corotate with a central gaseous disk limited by the dust lane (Rubin et al. 1997). NGC 4526 is a highly inclined SAB0⁰(s) galaxy in the Virgo cluster ($M_B = -20.7$). The stellar disk is not visible in the reconstructed image but is evident in the velocity and velocity dispersion fields. As in NGC 3384, the rotation on the major axis first increases, then decreases, and increases again in the outer parts, but the disk is much larger. It appears almost edge-on, giving rise to an elongated depression across the (hot) spheroid in the velocity dispersion map, and completely overwhelming the central peak.

NGC 4459 is another S0⁺(r) galaxy ($M_B = -20.0$) in Virgo. The same behavior as in NGC 3384 and NGC 4526 is observed along the major axis (see also Peterson 1978) but the minimum is shallower. The isovelocity contours are also less skewed, indicating a more face-on or intrinsically thicker disk (or both). This is supported by the absence of a clear disk signature in the velocity dispersion map. A statistical analysis of the entire SAURON sample will reveal the true fraction and necessary conditions for spheroids to harbor disks.

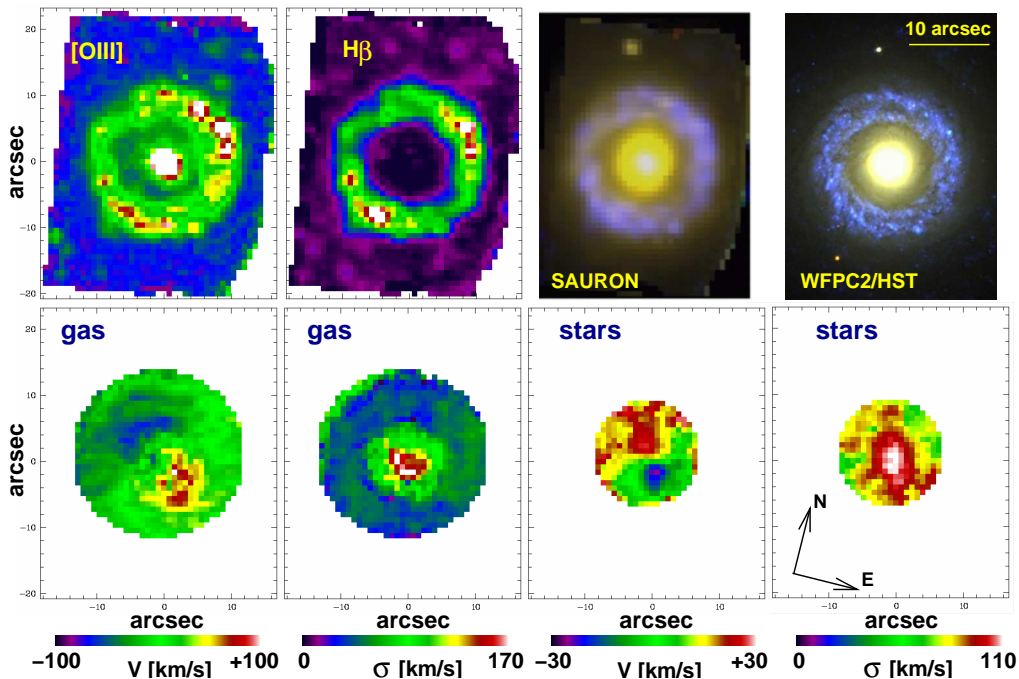


Figure 3. SAURON measurements of the stars and gas in NGC 7742 from one pointing with seeing $\approx 2''$. Top row: Emission-line intensity distributions of [OIII] and $H\beta$, followed by a reconstructed image composed of [OIII] and stellar continuum and a similar HST/WFPC2 image. Bottom row: Derived gas velocity and velocity dispersion fields, followed by the stellar velocity and velocity dispersion fields.

4. Gaseous Kinematics and Ionization Mechanisms

We now illustrate the scientific potential of the SAURON gaseous data. Paper II describes how the $H\beta$, [NI], and [OIII] emission lines are disentangled from the absorption lines by means of a spectral library and optimal template fitting. Results on the non-axisymmetric gaseous disks of NGC 3377 and NGC 5813 are presented in Papers I and II, respectively.

4.1. NGC 7742

NGC 7742 is a face-on Sb(r) spiral ($M_B = -19.8$) in a binary system and is among the latest spirals included in our sample. De Vaucouleurs & Buta (1980) identified the inner stellar ring; Pogge & Eskridge (1993) later detected a corresponding small, bright ring of HII regions with faint flocculent spiral arms. NGC 7742 possesses a large amount of HI, molecular gas, and dust (e.g. Roberts et al. 1991) and is classified as a LINER/HII object.

Figure 3 shows the [OIII] and $H\beta$ intensity maps, together with the derived velocity and velocity dispersion fields. Most of the emission is confined to a ring coinciding with the spiral arms. $H\beta$ dominates in the ring ($H\beta/[OIII] \approx 7 - 16$) but it is much weaker in the center ($H\beta/[OIII] \approx 1$). Also shown in Figure 3 is a reconstructed image composed of [OIII] and stellar continuum, and

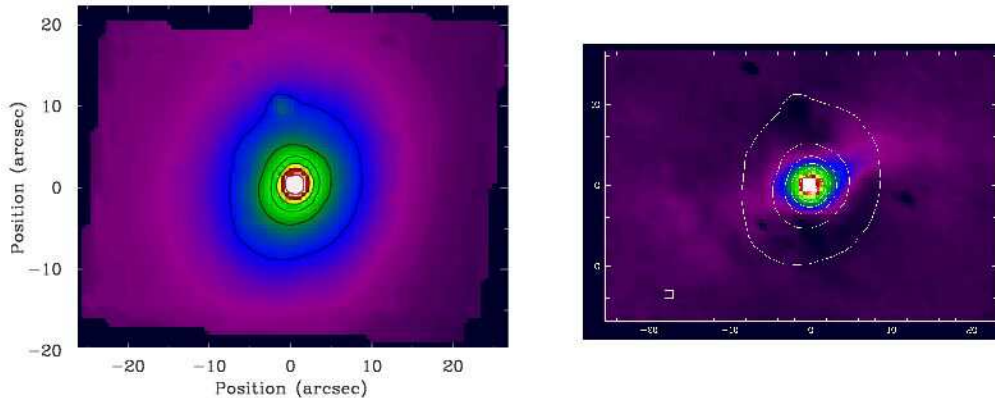


Figure 4. SAURON measurements of the stars and gas in NGC 4278, based on two pointings. Left: reconstructed stellar intensity. Right: [OIII] intensity. Isophotes are overlaid on both images. Scales are identical but fields-of-view differ slightly. The angular size of a SAURON lenslet is indicated in the bottom left corner of the [OIII] image.

a similar image composed of HST/WFPC2 exposures. The SAURON data does not have HST’s spatial resolution, but it does show that our algorithms yield accurate emission-line maps. The main surprise comes from the stellar and gas kinematics: the gas and stars within the ring are counter-rotating.

4.2. NGC 4278

NGC 4278 is an E1-2 galaxy ($M_B = -19.9$) in the Virgo cluster. It contains large-scale dust and a blue central point source (Carollo et al. 1997). Its stellar rotation curve is peculiar, rising rapidly at small distances from the nucleus and dropping to nearly zero beyond $r \approx 30''$ (Davies & Birkinshaw 1988; van der Marel & Franx 1993). NGC 4278 also contains a massive HI disk extending beyond $10 R_e$. The HI velocity field is regular but has non-perpendicular kinematic axes, indicating non-circular motions (Raimond et al. 1981; Lees 1992).

Figure 4 displays the reconstructed stellar intensity and [OIII] map obtained with SAURON. Despite the regular and well-aligned stellar isophotes, the distribution of ionized gas is very extended and strongly non-axisymmetric, similar to a bar terminated by ansae as observed in spiral galaxies. The gaseous bar is reminiscent of the dust structure observed at the center of Cen A (Mirabel et al. 1999), thought to have formed from the accretion of a gas-rich object, and could be linked to the active nucleus (LINER/Sy1) and compact radio core (Wrobel & Heeschen 1984). Again, observations of the entire SAURON sample will reveal the fraction of spheroids with ionized gas and its ionization and dynamical state.

5. Comparing SAURON and N-Body Data

With full knowledge of phase-space, N-body simulations can easily be projected and binned into three-dimensional data cubes. This allows an easy comparison with stellar kinematic data from integral-field spectrographs such as SAURON, without the intermediate step of deconvolution.

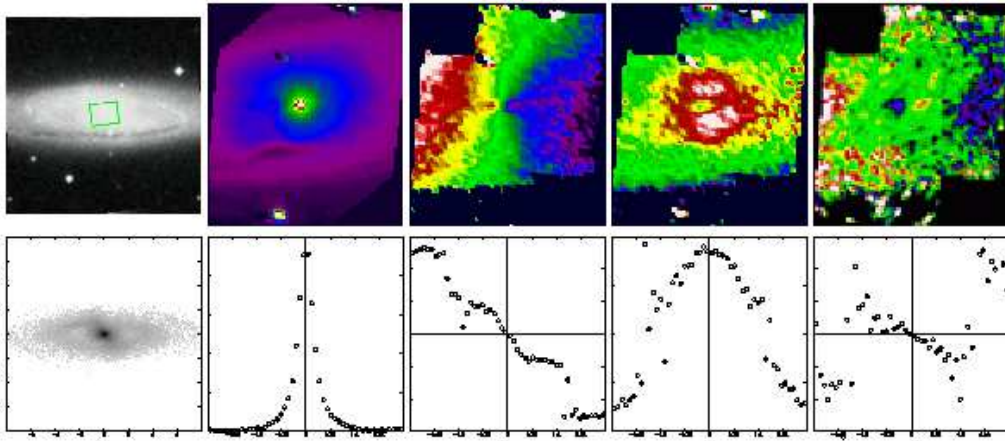


Figure 5. Comparison of SAURON observations with an N-body simulation. Top row: NGC 3623 large-scale image (Digitized Sky Survey), SAURON reconstructed total intensity, mean stellar velocity, velocity dispersion, and h_3 fields, from two pointings. A single SAURON footprint is overlaid on the DSS image (random orientation). Bottom row: Same for an N-body simulation, although only major axis profiles (cuts) are shown. The spatial axes of the N-body data were roughly scaled to NGC 3623; no attempt was made to scale the velocity data.

5.1. NGC 3623

In Figure 5, we compare SAURON observations of NGC 3623, a highly inclined SAB(rs)a galaxy in the Leo I Group ($M_B = -20.8$; Paper II and references therein), with a generic barred galaxy N-body simulation provided by E. Athanassoula (Athanassoula & Misiriotis 2002; see also Bureau & Athanassoula, in prep.). This is for illustration purposes only, as no attempt was made to match either a timestep or specific simulation with the observations. A viewing angle was roughly estimated by eye. The line-of-sight velocity profiles extracted from the simulations were fitted with the same algorithm as the observations (the latter after deconvolution with FCQ), allowing a direct comparison, but only major axis profiles were extracted due to low S/N.

The rotation curve disk signature discussed above is clearly seen in both datasets, but the simulation only shows a flattening of the dispersion in the center, not a dip, and the h_3 profile is correlated (rather than anti-correlated) with V in the inner parts. This suggests that the N-body central component is dynamically hot and rather elongated, contrary to the central stellar disk of NGC 3623. It remains to be seen if this is due to x_2 orbits. The simulation also suggests that dissipation may indeed be necessary to create the many stellar disks observed by SAURON in spheroids.

Acknowledgments. Support for this work was provided by NASA through Hubble Fellowship grant HST-HF-01136.01 awarded by the Space Telescope Science Institute, which is operated by the Association of Universities for Research in Astronomy, Inc., for NASA, under contract NAS 5-26555.

References

- Athanassoula, E., & Misiriotis, A. 2002, *MNRAS*, 330, 35
- Bacon, R., et al. 1995, *A&AS*, 113, 347
- Bacon, R., et al. 2001, *MNRAS*, 326, 23 (Paper I)
- Bacon, R., et al. 2002, in *Galaxies: The Third Dimension*, eds. M. Rosado, L. Binette, & L. Arias (San Francisco: ASP), in press.
- Barnes, J. E. 1998, in *Galaxies: Interactions and Induced Star Formation*, eds. D. Friedli, L. Martinet, & D. Pfenniger (Berlin: Springer), 275
- Bender, R. 1990, *A&A*, 229, 441
- Bender, R., & Nieto, J.-L. 1990, *A&A*, 239, 97
- Birkinshaw, M., & Davies, R. L. 1985, *ApJ*, 291, 32
- Busarello, G., Capaccioli, M., D'Onofrio, M., Longo, G., Richter, G., & Zaggia, S. 1996, *A&A*, 314, 32
- Caon, N., Macchetto, F. D., & Pastoriza, M. 2000, *ApJS*, 127, 39
- Carollo, C. M., Franx, M., Illingworth, G. D., & Forbes, D. 1997, *ApJ*, 710
- Cretton, N., Rix, H.-W., & de Zeeuw, P. T. 2000, *ApJS*, 536, 319
- Davies, R. L., & Birkinshaw, M. 1988, *ApJS*, 68, 409
- Davies, R. L., et al. 2001, *ApJ*, 548, L33
- Davies, R. L., Sadler, E. M., & Peletier, R. F. 1993, *MNRAS*, 262, 650
- Dressler, A. 1980, *ApJ*, 236, 351
- Efstathiou, G., Ellis, R. S., & Carter, D. 1982, *MNRAS*, 201, 975
- Eggen, O. J., Lynden-Bell, D., & Sandage, A. R. 1962, *ApJ*, 136, 748
- Emsellem, E., et al. 2002, in *Galaxies: The Third Dimension*, eds. M. Rosado, L. Binette, & L. Arias (San Francisco: ASP), in press.
- Faber, S. M., et al. 1997, *AJ*, 114, 1771
- Fisher, D. 1997, *AJ*, 113, 950
- Gorgas, J., Efstathiou, G., & Aragon-Salamanca, A. 1990, *MNRAS*, 245, 217
- Gonzalez, J. J. 1993, PhD Thesis, Univ. of California at Santa Cruz
- Lees, J. F. 1992, PhD Thesis, Princeton University
- van der Marel, R. P., & Franx, M. 1993, *ApJ*, 407, 525
- Mirabel, I. F., et al. 1999, *A&A*, 341, 667
- Naab, T., Burkert, A., & Hernquist, L. 1999, *ApJ*, 523, L133
- Peterson, C. J. 1978, *ApJ*, 222, 84
- Pogge, R. W., & Eskridge, P. B. 1993, *AJ*, 106, 1405
- Raimond, E., Faber, S. M., Gallagher, J.S., & Knapp, G.R. 1981, *ApJ*, 246, 708
- Roberts, M., et al. 1991, *ApJS*, 75, 751
- Rubin, V. C., Kenney, J. D. P., & Young, J. S. 1997, *AJ*, 113, 1250
- Searle, L., & Zinn, R. 1978, *ApJ*, 225, 357
- de Vaucouleurs, G., & Buta, R. 1980, *AJ*, 85, 637
- Worthey, G., Faber, S. M., Gonzalez, J. J., & Burstein, D. 1994, *ApJS*, 94, 687
- Wrobel, J. M., & Heeschen, D. S. 1984, *ApJ*, 287, 41
- de Zeeuw, P. T., et al. 2002, *MNRAS*, 329, 513 (Paper II)